M. Mendizabal, A. McCloskey, S. Zarate and J. Poza, "Fast and Accurate Vibration Response Calculation Procedure for Permanent Magnet Synchronous Machines," 2022 International Conference on Electrical Machines (ICEM), Valencia, Spain, 2022, pp. 2207-2213.

DOI: https://doi.org/10.1109/ICEM51905.2022.9910849

Fast and Accurate Vibration Response Calculation Procedure for Permanent Magnet Synchronous Machines

M. Mendizabal, A. McCloskey, S. Zarate, J. Poza

Abstract – **The vibration of the stator frame due to electromagnetic forces is one of the main noise and vibration sources of electric machines. In some applications, due to the wide variety of working conditions, design optimizations are not enough, and the control of the machine is needed to reduce vibrations. Therefore, this work presents a reduced model, to be used during the control, which is able to estimate the stator frame vibrations of a Permanent Magnet Synchronous Machine. Finite Element calculations are performed, and the results are saved in Look-Up Tables and implemented in a calculation procedure, allowing a fast and accurate vibration estimation for any input conditions. The proposed model is validated using Finite Element simulations, and it is concluded that it offers high accuracy with a calculation time of a few seconds. Thus, the model developed is suitable to be further developed and implemented in a control procedure.**

Index Terms— **Electric machines, Electromagnetic modeling, Finite Element analysis, Metamodeling, Numerical simulation, Permanent magnet machines, Table lookup, Vibrations.**

I. Introduction

PERMANENT Magnet Synchronous Machines (PMSM) are used in a wide variety of applications, due to their high torque density [1], [2]. In most applications, the comfort of the users is becoming a critical requirement, and thus, it is essential to optimize the vibrational response of the machines. Among all the sources of noise and vibration, the vibrations of the stator and the frame generated by electromagnetic forces are one of the most critical ones [2].

In literature, several approaches were presented to optimize the vibration response of PMSMs by design improvements [3]. However, due to the wide operation range required in many applications, it is very complex to stablish an optimum design for all working conditions [4], [5]. Therefore, an alternative approach is to reduce the vibrations by means of control.

Many control methods performed in literature act based on measurements provided by accelerometers or other external actuators [6], [7], which increases the cost and complexity of the control. In order to avoid the use of additional elements, a model to estimate the vibration of the machine can be used, instead of measuring it.

In order to obtain an accurate estimation of the vibrations of the stator, a multi-physical model needs to be developed. An electromagnetic model is needed to estimate the radial forces produced by electromagnetic phenomena, and a structural model is needed to estimate the dynamic response produced by those forces [8].

In [9], a Finite Element (FE) model of a permanent magnet DC motor was presented, and the structural vibrations and acoustic noise generated by the motor were estimated. In [10] and [11], a similar methodology was implemented for induction motors, and in [12] for a switched reluctance motor. In [1], [2] and [13], numerical models to estimate the vibrations and noise of PMSMs were presented and validated.

As demonstrated in those works, Finite Element Method (FEM) is a very accurate tool that can be used for any machine typology, but its computational cost is too high to be used in a dynamic control.

On the other hand, analytical models offer fast calculations. In [14] and [15], analytical expressions for the electromagnetic forces in PMSMs were presented. In [16], an analytical model to calculate the vibrational response of an electrical motor was developed.

However, despite their fast response, the accuracy of analytical models is, generally, not high enough, due to the simplifications that are performed.

In order to develop an effective control, the accuracy of FEM is required, with a short enough calculation time. None of the calculation procedures found in literature offers the accuracy of the FE simulations with a low computational time. Therefore, a new procedure to estimate vibration is needed, to obtain the accuracy of the FE models, but with a computational effort low enough to be calculated in real time.

In this work, a new calculation procedure employing surrogated models is proposed to fulfil the mentioned requirements. Complex FE models were created, and simulations were performed in a wide range of conditions. The results of the simulations were gathered in Look-Up Tables (LUT) (and implemented in the model), creating a fast and simple tool that accurately provides the output result for any input variables.

In [17] and [18], FE analyses were performed to estimate the electromagnetic torque for different current and rotor position values. The results were saved as LUTs and introduced to the models, avoiding FE calculations in the control procedure.

In this work, a similar approach is proposed, and FE simulations are performed to generate a LUT that relates the

The Basque Government (VEGAN KK21-0044 and predoctoral grant) and the Provincial Council of Gipuzkoa (NVHCONTROL) financially supported this research.

electromagnetic pressure on the teeth with current and rotor position.

Another reduced model is used to describe the mechanical behaviour of the machine. FE simulations are performed to calculate the natural frequencies and vibration modes of the machine. The results are saved as LUTs, in order to allow a fast estimation of the vibration of the stator due to the pressure on the teeth.

In section II. , the calculation procedure is described. A detailed explanation of the electromagnetic and structural models is given, and the FE simulations performed to obtain the LUTs are described. In section III. , the calculation procedure is validated, by comparing the vibrational response estimated by the model to the response obtained in FE simulations.

II. Model of the Machine

The model of the PMSM described in Table I is developed and implemented in the Matlab/Simulink simulation platform.

TABLE I
MAIN CHARACTERISTICS OF THE MACHINE

Number of slots	Number of pole pairs	Number of winding layers
36	15	2

Fig. 1 shows an overview of the workflow of the model. The inputs are the rotational speed of the machine and the current in *dq* axes. First, in the electromagnetic model, the electromagnetic pressure on the stator teeth surface is obtained. Then, the pressure is used as the input of the structural model to calculate the vibration at the surface of the stator frame.

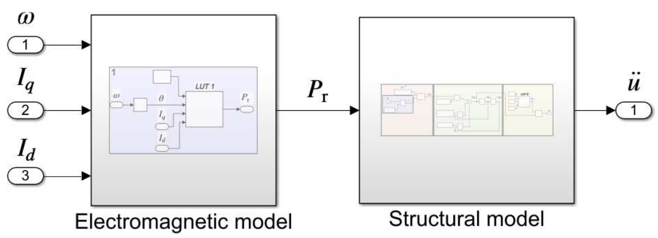

Fig. 1. Overview of the whole model

A. Electromagnetic Model

The electromagnetic model consists on the creation of a LUT that relates the rotor position and the current introduced to the machine with the magnetic pressure on the stator teeth.

The radial (P_r) and tangential (P_t) components of the magnetic pressure are obtained using Maxwell's tensor [19]:

$$P_r = \frac{B_r^2 - B_t^2}{2\mu_0}$$
$$P_t = \frac{B_r B_t}{\mu_0} \tag{1}$$

where B_r and B_t are the radial and tangential components of the magnetic flux density and μ_0 is the magnetic permeability of the air.

It is assumed that the vibrations of the frame mainly occur due to the radial component of the pressure, and that the tangential component does not have a considerable impact [19]. Therefore, in order to simplify the model and reduce the computational cost, only the radial pressure is considered in the calculation procedure.

To apply Maxwell's tensor, the magnetic flux density in the internal surface of the teeth needs to be known, for any current and rotor position. In order to do so, a 2D FE model of the machine was created in a FE software, and a simulation sweep for different working conditions of the machine was performed.

The model is defined as explained in [20]. The simulations were performed in the following working conditions:

- I_d : [-3; -2; -1; -0.8; -0.6; -0.4; -0.2; 0; 0.2; 0.4; 0.6; 0.8; 1; 2; 3] A (*rms*)
- I_q : [-13.3; -9; -6.5; -4; -2; -1.5; -1; -0.8; -0.6; -0.4; -0.2; 0; 0.2; 0,4; 0.6; 0.8; 1; 1.5; 2; 4; 6.5; 9; 13.3] A (*rms*)

Assuming the machine ideal, and as it has three winding periodicities, it is not necessary to perform the simulations for the entire machine. To reduce the computational cost, just one winding periodicity was considered, which corresponds to the third part of the machine, and the results were then repeated three times to complete the entire machine.

As it is a magnetostatic calculation, each time increment refers to a certain position of the rotor (θ). The resolution of the rotor position is defined by the maximum temporal electrical order ($r_{\max}$) that can be correctly analysed without aliasing.

The minimum amount of rotor positions (N_θ) can be defined by equation (2).

$$N_\theta = r_{\max} pk \tag{2}$$

where p the number of pole pairs and k the number of points per period needed to correctly define each frequency order. In accordance with equation (2), in order to represent the 30th temporal electric order and considering 6 points per period, a minimum amount of 2700 rotor positions was defined.

In this work, the harmonics introduced by PWM were not analysed. PWM introduces high frequency components to the current, up to several kHz, resulting in much higher temporal electric orders than the maximum stablished. Therefore, a much higher resolution would be necessary for the rotor position, which would considerably increase the required time to perform the simulations and obtain the electromagnetic LUT.

Apart from that, the sample time used in the reduced model would need to be much smaller in order to consider the high frequency harmonics of the current, which would make the calculation much slower.

Moreover, in order to obtain the spatial distribution of the pressure for every rotor position, a path was defined along the stator teeth.

In this case, when defining the path, the number of points per tooth (N_t) defines the maximum spatial electrical order (s_{max}) that can be correctly estimated without aliasing.

$$N_t = \frac{\alpha_t s_{max} p k}{2\pi} \tag{3}$$

where α_t is the angle of a tooth. According to equation (3), in order to represent the 30th spatial electric order, and considering 6 points per period, a minimum number of 40 points per tooth is needed.

In each simulation, the radial and tangential components of the magnetic flux density (B_r and B_t) were exported, for all the points defined in the path, for each rotor position.

The data was gathered in the matrices $B_r(I_d, I_q, \theta, \alpha)$ and $B_t(I_d, I_q, \theta, \alpha)$, where θ is the rotor position and α is the spatial tangential position. Then, applying Maxwell's tensor, the radial pressure matrix $P_r(I_d, I_q, \theta, \alpha)$ was obtained and implemented as LUT 1 in the electromagnetic model (Fig. 2).

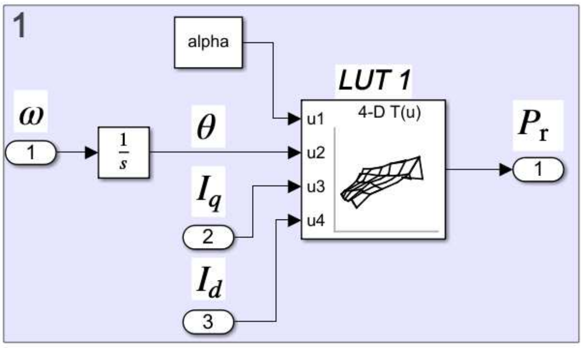

Fig. 2. Electromagnetic model

B. *Structural Model*

Starting with the pressure on the surface of the teeth obtained by the electromagnetic model, the structural model is defined to calculate the vibration of the stator frame.

The calculation procedure is developed in accordance with the equation of the motion of the mechanical system:

$$[M]\{\ddot{u}\} + [C]\{\dot{u}\} + [K]\{u\} = \{f\} \tag{4}$$

where $[M]$, $[C]$ and $[K]$ are the mass, damping and stiffness matrices, $\{u\}$ is the displacement vector and $\{f\}$ the force vector.

Solving the previous equation in the matrix form is very time consuming. However, the equation system can be decoupled by applying the modal superposition method, which considers that the motion is the result of the contribution of the vibration modes of the system. According to this method, the response of the system is the product of the mode shape matrix $[U]$ and the modal amplitude vector $\{\eta\}$:

$$\{u\} = [U]\{\eta\} \tag{5}$$

If the transpose of the mode shape matrix is pre-multiplied to all the elements, the equation of the motion is written as:

$$\begin{aligned}&[U]^T[M][U]\{\ddot{\eta}\} + [U]^T[C][U]\{\dot{\eta}\} + \\ &[U]^T[K][U]\{\eta\} = [U]^T\{f\}\end{aligned} \tag{6}$$

Assuming that the damping of the system can be modelled with modal damping, the equation can be written using the modal mass, modal damping and modal stiffness matrices.

$$[M_k]\{\ddot{\eta}\} + [C_k]\{\dot{\eta}\} + [K_k]\{\eta\} = \{f_k\} \tag{7}$$

where $[M_k]$, $[C_k]$ and $[K_k]$ are diagonal matrices, being all the non-diagonal elements equal to zero. The k-th elements of the diagonals (m_k, c_k, k_k), correspond to the modal mass, modal damping and modal stiffness of mode k.

Therefore, the equation system can be decoupled, and a set of differential equations, equal to the number of modes considered in the analysis, is obtained:

$$m_k\ddot{\eta}_k + c_k\dot{\eta}_k + k_k\eta_k = f_k \tag{8}$$

By dividing all the terms by the modal mass, and knowing that $c_k = 2\xi_k\omega_k m_k$ and $k_k = \omega_k^2 m_k$, the equation is rewritten as:

$$\ddot{\eta}_k + 2\xi_k\omega_k\dot{\eta}_k + \omega_k^2\eta_k = f_k / m_k \tag{9}$$

where ξ_k and ω_k are the damping ratio and the natural frequency (in rad/s) of mode k. f_k is the effective force on mode k, and it is the scalar product of the modal shape of that mode and the spatial distribution of the force vector.

$$f_k = \{U_k(\theta)\}\{f(\theta)\} \tag{10}$$

The closer the spatial distribution of the force is to the shape of a mode, the higher the contribution of that mode to the vibration will be.

The differential equation is solved for each mode and the modal amplitude vector is obtained.

Then, equation (5) is used to obtain the vibrational response of the system. Multiplying the mode shape matrix with the modal amplitude vector, the acceleration in any point of the motor is obtained for each mode. Summing the response of all modes, the total vibrational response is obtained, for any axial (x) and tangential (θ) position.

$$u(x,\theta,t) = \sum_{k=1}^{\infty} U_k(x,\theta)\eta_k(t) \tag{11}$$

Fig. 3. shows the structural model developed in this work, which is divided in four steps. The model is defined in accordance with the calculation procedure explained in the previous paragraphs, and in order to calculate the mode shape matrices that are necessary for the calculations, a FE model of the machine was created in the ABAQUS software. The model is defined as explained in [21].

1) *Calculation of the Force Vector*

The pressure obtained from the electromagnetic model is used as the input of the structural model. The pressure is converted into the force vector $\{f\}$, by considering the area that corresponds to each of the points of the structural mesh.

$$\{f\} = \frac{P_r}{R\Delta L\,\Delta\alpha} \tag{12}$$

where R is the inner radius of the stator, and ΔL and $\Delta\alpha$ are the axial and angular resolution of the mesh.

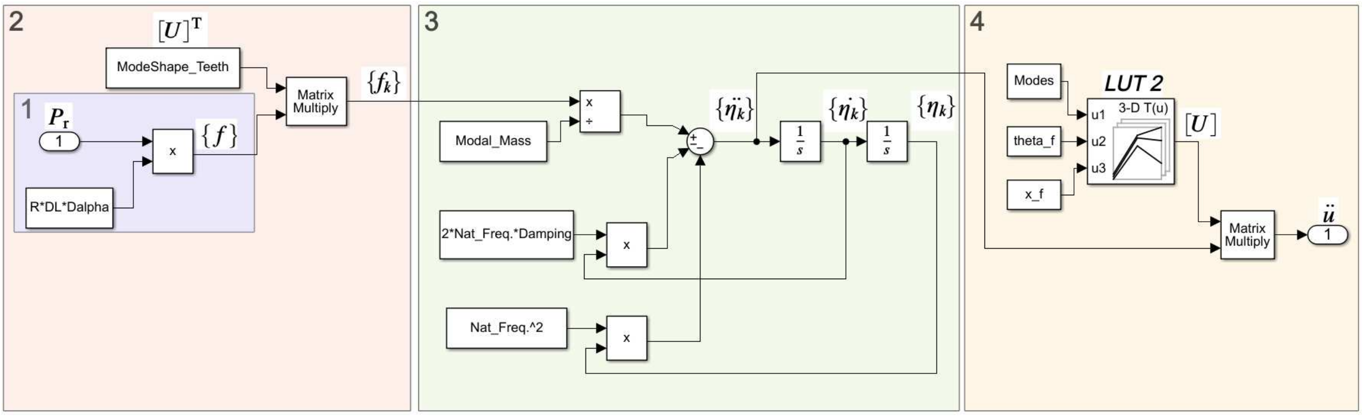

Fig. 3. Structural model

2) Calculation of the Effective Force Vector

Using the FE model, the vibration modes of the system are calculated, in order to obtain the mode shape matrix that is needed to calculate the effective force vector $\{f_k\}$.

When the modal superposition method is considered, it is convenient to calculate the modes for at least twice the frequency range of interest for the response, as higher frequency modes may also have a considerable influence on lower frequencies. In this work, the upper limit for the response is the 30$^{\text{th}}$ electric order, and all the modes within 5 times that frequency range were calculated. Even though less modes would probably be enough for an accurate calculation, the number of modes chosen allows a sufficiently fast calculation. However, an analysis of the reduction of the number of modes considered should be done in the future to minimize the calculation time.

The vibration modes contain the movement of every single point of the model, but in order to develop equation (10) and calculate the effective force vector, only the mode shape of the stator teeth surface (the area in which the force is applied) is required.

As mentioned in section II. A. , the number of points per tooth defines the maximum spatial electrical order that can be correctly estimated without aliasing. According to equation (3), a minimum number of 40 points per tooth is needed to reach the 30$^{\text{th}}$ spatial electric order.

Fig. 4 shows, as an example, the shape of a specific vibration mode in one tooth. The movement of each node is obtained as the difference between its deformed and undeformed position.

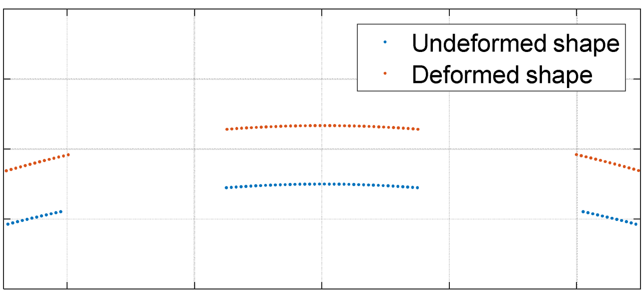

Fig. 4. Shape of a specific vibration mode

In step-skewed rotors, the magnetic pressure is not constant along the axial direction of the stator. For that reason, a 3D electromagnetic model would be needed to consider the axial distribution of the pressure, which would increase considerably the required time to obtain the electromagnetic LUT.

As the machine analysed in this work has a non-skewed rotor, the pressure is constant along the axial direction of the stator, which is the reason why a 2D electromagnetic model was used.

However, as the machine is not axially symmetrical, the modal shapes vary in that direction. Therefore, 5 axial sections were defined in the stator, and for each axial position, a path or point group was defined along the edge of the stator teeth. Then, for every mode, a vector containing the motion of all the points in each path was exported. Only the radial component of the motion was exported, as the tangential component of the pressure was neglected.

The results for the mode shapes of the teeth are organized as shown in Fig. 5. Each column represents a mode and each row a tangential (θ) and axial (x) position.

Vibration modes

Tangential (θ) and axial (x) position

$U_1(\theta_1,x_1)$	$U_2(\theta_1,x_1)$	...	$U_k(\theta_1,x_1)$
$U_1(\theta_2,x_1)$	$U_2(\theta_2,x_1)$	...	$U_k(\theta_2,x_1)$
...	...	...	...
$U_1(\theta_n,x_1)$	$U_2(\theta_n,x_1)$	...	$U_k(\theta_n,x_1)$
$U_1(\theta_1,x_2)$	$U_2(\theta_1,x_2)$	...	$U_k(\theta_1,x_2)$
$U_1(\theta_2,x_2)$	$U_2(\theta_2,x_2)$	...	$U_k(\theta_2,x_2)$
...	...	...	...
$U_1(\theta_n,x_2)$	$U_2(\theta_n,x_2)$	...	$U_k(\theta_n,x_2)$
...	...	...	...
$U_1(\theta_1,x_m)$	$U_2(\theta_1,x_m)$	...	$U_k(\theta_1,x_m)$
$U_1(\theta_2,x_m)$	$U_2(\theta_2,x_m)$	...	$U_k(\theta_2,x_m)$
...	...	...	...
$U_1(\theta_n,x_m)$	$U_2(\theta_n,x_m)$	...	$U_k(\theta_n,x_m)$

Fig. 5. Mode shape matrix exported from ABAQUS

3) Resolution of the Differential Equation

In the third step of the procedure, equation (9) is solved, and the modal amplitude response vector h_k is obtained. The modal mass vector, which needs to be divided to the effective force, was also exported from the FE software.

4) Calculation of the Vibration on the Stator Frame

Finally, the vibration on the external surface of the stator is calculated using equation (11). In this step, the mode shape matrix of the stator frame is required, and it was obtained from the same FE calculation of section II. B.

In order to obtain the response at any point of the frame or to visualize the movement of the entire frame, the matrices for all the nodes in the external surface of the stator should be exported. However, in order to lighten the model (to be used in a control procedure), it would be enough to export the matrices for a small number of representative points.

Once the results were exported, they were organized to create the LUT 2 of Fig. 3. The LUT offers the mode shape matrix of any tangential (θ_f) and axial (x_f) position of the frame. Multiplying the values of the mode shapes at the point of interest with the modal amplitude vector, and summing the results obtained for all the modes, the vibration of that specific point of the frame is obtained.

III. Validation of the Model

In order to validate the simulation procedure presented in this work, two cases were simulated by FE calculations.

The validation was performed by comparing the vibration response obtained in the FE simulations to the response estimated by the proposed reduced model running in Simulink. The central point of the upper face of the stator frame was chosen as the reference point.

Both in the reduced model and in the FE calculation, the response until 0.5 s was calculated, with a time increment of $5 \cdot 10^{-6}$ s.

A. Validation of the Structural Model

First, in order to validate the structural model, an impulse was introduced to the mechanical system. An instantaneous unitary pressure (1 Pa) was created and applied to the surface of all the stator teeth. In this case, the electromagnetic models are not considered.

Introducing an impulse to the machine, a transient response is obtained, which is attenuated along the time. Fig. 6 shows the acceleration obtained in the reference point, both in the reduced model and by the FE simulation, in the frequency domain.

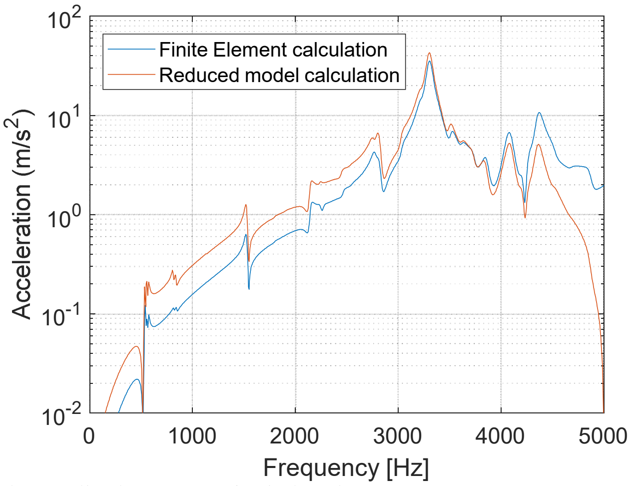

Fig. 6. Vibration response for the impulse case

The reduced model slightly overestimates the vibration response calculated in the FE simulation. The frequencies where the peaks arise are well estimated, and the trend of the curves is the same. The amplitudes are not the same, but differences are generally small.

B. Validation of the Complete Model

A second simulation was performed to validate the complete model presented in this work. In this case, a real functioning case was simulated, with a rotational speed of 300 rpm and an I_q current of 9 A (*rms*).

First, the selected current and rotational speed were introduced to the electromagnetic FE model, and the spatial distribution of the pressure on the teeth was exported. Then, that pressure was used as the input for the structural FE model, where the vibrational response of the machine was calculated.

As the current is maintained in time, once the transient response is attenuated, a steady-state response is obtained.

Fig. 7 shows the acceleration obtained in the reference point in the frequency domain, in the transient region. As in the case of the impulse, the estimation of the general trend and the peak frequencies is accurate, even though some differences are observed regarding the amplitudes.

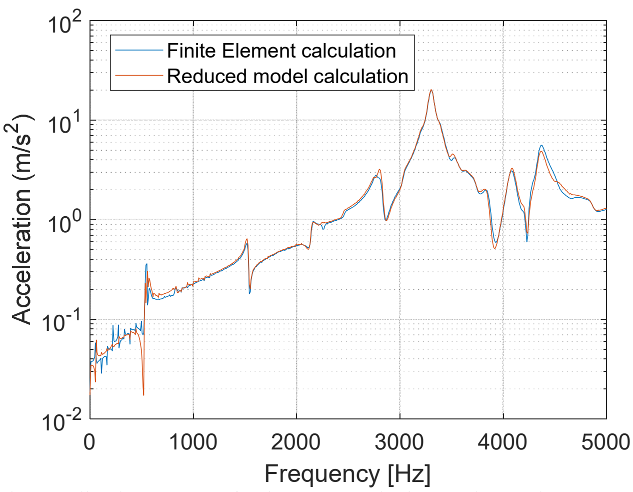

Fig. 7. Vibration response for the Iq 9 case, in the transient region

Fig. 8 shows the acceleration in the steady-state region. The amplitude of most frequency orders is estimated accurately, even though some differences are observed in several harmonics.

There may be several reasons to explain the differences in the amplitudes. On the one hand, regarding the FE simulations, the electromagnetic pressure calculated in the FE electromagnetic software is applied to the FE structural model, and a certain error might be committed in that transmission. The structural FE software converts the pressure on the stator teeth surface into forces, distributing it in all the nodes defined in the mesh of the surface. Depending on the size of the elements, some information may be lost. For this reason, in the future, it should be analysed how the vibration response changes if the mesh is modified.

On the other hand, concerning the reduced model, an error might be committed due to the axial discretization defined for the mode shape matrix of the stator teeth surface. If there are vibration modes with a significant axial deformation, exporting the modal shape of only 5 sections might not be enough. Thus, it should be studied how the vibration response changes considering a higher number of axial sections.

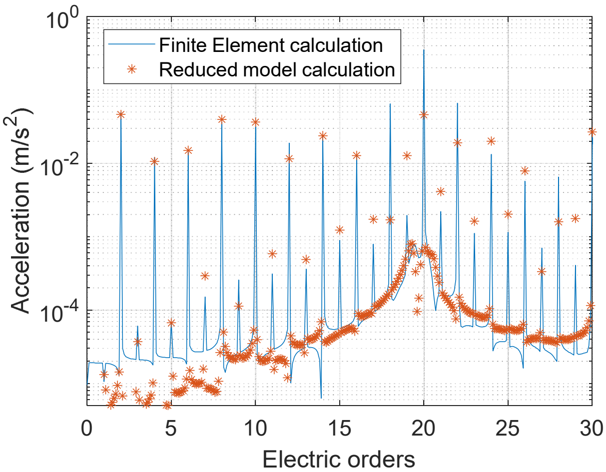

Fig. 8. Vibration response for the Iq 9 A case, in the steady-state region

The electromagnetic FE simulation requires a computational time of 5 days in a 12 core and 96 GB RAM computer and the structural 36 hours. In contrast, the calculation was performed in 50 seconds by the reduced model in Simulink.

In order to perform an accurate enough comparison, a very small time increment was used for the validation. However, it has to be analysed which would be the optimum time increment, so that the calculation time is reduced without compromising the accuracy of the results.

IV. Conclusions

This work presents a reduced model to estimate the vibration response on the stator frame of PMSMs in a fast and accurate way. An electromagnetic model and a structural model were created, both based on LUTs that gather the information obtained in complex and time-consuming FE simulations.

The validation shows that the transient and steady-state response of the machine are estimated accurately. The same trend as in FE calculations is observed, and the differences in amplitudes are generally small. A reason for those differences might be the error committed in the structural FE software when distributing the magnetic pressure as a force to each node of the mesh. Another reason might be that an insufficient number of axial sections was set to export the modal shape matrix of the stator teeth. To fully comprehend the reason and minimize the differences in the results, these two phenomena should be furtherly analysed.

The model presented in this work reduces the calculation time of a regular FE analysis from several days to a few seconds, without compromising the accuracy of the results. For that reason, this model could be suitable to be implemented on an active control system in the future. For that, the model needs to be optimized, as the calculation time needs to be reduced. There are several parameters that should be further studied: the time increment of the model, the number of elements of the LUT used in the electromagnetic model, the number of vibration modes considered and the number of representative nodes for the mode shapes.

V. References

[1] K. Qian, J. Wang, Y. Gao, Q. Sun, and J. Liang, "Interior noise and vibration prediction of permanent magnet synchronous motor," *Journal of Vibroengineering*, vol. 20, no. 5, pp. 2225–2236, Aug. 2018, doi: 10.21595/jve.2018.18605.

[2] D. Torregrossa, F. Peyraut, B. Fahimi, J. Mboua, and A. Miraoui, "Multiphysics finite-element modeling for vibration and acoustic analysis of permanent magnet synchronous machine," *IEEE Transactions on Energy Conversion*, vol. 26, no. 2, pp. 490–500, Jun. 2011, doi: 10.1109/TEC.2010.2080681.

[3] C. Gan, J. Wu, Q. Sun, W. Kong, H. Li, and Y. Hu, "A Review on Machine Topologies and Control Techniques for Low-Noise Switched Reluctance Motors in Electric Vehicle Applications," *IEEE Access*, vol. 6. Institute of Electrical and Electronics Engineers Inc., pp. 31430–31443, 2018. doi: 10.1109/ACCESS.2018.2837111.

[4] M. Kawa, K. Kiyota, J. Furqani, and A. Chiba, "Acoustic Noise Reduction of a High-Efficiency Switched Reluctance Motor for Hybrid Electric Vehicles with Novel Current Waveform," *IEEE Transactions on Industry Applications*, vol. 55, no. 3, pp. 2519–2528, May 2019, doi: 10.1109/TIA.2018.2888847.

[5] L. Kang, J. Xia, H. Su, Z. Li, and S. Liu, "On-line Control Strategy for Radial Vibration Suppression of PMSM by Multi- harmonic Current Injection Method," *IEEE Transactions on Industrial Electronics*, pp. 1–1, Oct. 2021, doi: 10.1109/tie.2021.3106027.

[6] A. J. den Hamer, G. Z. Angelis, and N. B. Roozen, "Broad-band active vibration suppression using PPF focused on industrial application," *IEEE/ASME Transactions on Mechatronics*, vol. 10, no. 2, pp. 146–153, Apr. 2005, doi: 10.1109/TMECH.2005.844718.

[7] X. Ojeda, X. Mininger, H. ben Ahmed, M. Gabsi, and M. Lécrivain, "Piezoelectric actuator design and placement for switched reluctance motors active damping," *IEEE Transactions on Energy Conversion*, vol. 24, no. 2, pp. 305–313, 2009, doi: 10.1109/TEC.2009.2016146.

[8] J. le Besnerais, "Fast Prediction of Variable-Speed Acoustic Noise due to Magnetic Forces in Electrical Machines," *2016 XXII International Conference on Electrical Machines (ICEM)*, 2016, doi: 10.1109/ICELMACH.2016.7732836.

[9] M. Furlan, A. Černigoj, and M. Boltežar, "A coupled electromagnetic-mechanical-acoustic model of a DC electric motor," *COMPEL - The International Journal for Computation and Mathematics in Electrical and Electronic Engineering*, vol. 22, no. 4, pp. 1155–1165, 2003, doi: 10.1108/03321640310483075.

[10] S. Rainer, O. Bíró, B. Weilharter, and A. Stermecki, "Weak coupling between electromagnetic and structural models for electrical machines," in *IEEE Transactions on Magnetics*, Aug. 2010, vol. 46, no. 8, pp. 2807–2810. doi: 10.1109/TMAG.2010.2043827.

[11] S. Sathyan, U. Aydin, and A. Belahcen, “Acoustic Noise Computation of Electrical Motors Using the Boundary Element Method,” *Energies 2020, Vol. 13, Page 245*, vol. 13, no. 1, p. 245, Jan. 2020, doi: 10.3390/EN13010245.

[12] C. G. C. Neves, R. Carlson, N. Sadowski, J. P. A. Bastos, N. S. Soeiro, and S. N. Y. Gerges, “Calculation of Electromagnetic-Mechanic-Acoustic Behavior of a Switched Reluctance Motor,” *IEEE Transactions on Magnetics*, vol. 36, no. 4, pp. 1364–1367, 2000, doi: 10.1109/20.877692.

[13] J. B. Dupont, R. Aydoun, and P. Bouvet, “Simulation of the noise radiated by an automotive electric motor: Influence of the motor defects,” *SAE International Journal of Alternative Powertrains*, vol. 3, no. 2, pp. 310–320, Jul. 2014, doi: 10.4271/2014-01-2070.

[14] S. Huang, M. Aydin, and T. A. Lipo, “Electromagnetic Vibration and Noise Assessment for Surface Mounted PM Machines,” in *2001 Power Engineering Society Summer Meeting.*, 2001, vol. 224. doi: 10.1109/PESS.2001.970284.

[15] M. Mendizabal, A. McCloskey, J. Poza, S. Zarate, J. Iriondo, and L. Irazu, “Optimum slot and pole design for vibration reduction in permanent magnet synchronous motors,” *Applied Sciences (Switzerland)*, vol. 11, no. 11, Jun. 2021, doi: 10.3390/app11114849.

[16] A. McCloskey, X. Arrasate, X. Hernández, I. Gómez, and G. Almandoz, “Analytical calculation of vibrations of electromagnetic origin in electrical machines,” *Mechanical Systems and Signal Processing*, vol. 98, pp. 557–569, Jan. 2018, doi: 10.1016/j.ymssp.2017.04.050.

[17] Y. Kano, K. Watanabe, T. Kosaka, and N. Matsui, “A novel approach for circuit-field-coupled time-stepping electromagnetic analysis of saturated interior PM motors,” *IEEE Transactions on Industry Applications*, vol. 45, no. 4, pp. 1325–1333, 2009, doi: 10.1109/TIA.2009.2023391.

[18] X. Chen, J. Wang, B. Sen, P. Lazari, and T. Sun, “A high-fidelity and computationally efficient model for interior permanent-magnet machines considering the magnetic saturation, spatial harmonics, and iron loss effect,” *IEEE Transactions on Industrial Electronics*, vol. 62, no. 7, pp. 4044–4055, Jul. 2015, doi: 10.1109/TIE.2014.2388200.

[19] P. Pennacchi, “Computational model for calculating the dynamical behaviour of generators caused by unbalanced magnetic pull and experimental validation,” *Journal of Sound and Vibration*, vol. 312, no. 1–2, pp. 332–353, Apr. 2008, doi: 10.1016/j.jsv.2007.10.052.

[20] S. Zarate, A. Egea, G. Almandoz, A. Mccloskey, U. Galfarsoro, and A. Urdangarin, “A study of the effects of the magnetization tolerance in the manufacturing process on permanent magnet synchronous machines,” *2020 10th International Electric Drives Production Conference, EDPC 2020 - Proceedings*, Dec. 2020, doi: 10.1109/EDPC51184.2020.9388212.

[21] A. McCloskey, X. Arrasate, X. Hernandez, and O. Salgado, “Measurement and simulation of the vibroacoustic performance of an electric motor,” *Mechanisms and Machine Science*, vol. 23, pp. 339–348, 2015, doi: 10.1007/978-3-319-09918-7_30/FIGURES/8.

VI. Biographies

Mikel Mendizabal was born in Zumaia, Spain. He received the B.Sc. and M.Sc. degrees in Mechanical Engineering and Industrial Engineering from Mondragon Unibertsitatea in 2019 and 2021 respectively.

Since 2021, he has been with the Electronics department of the Faculty of Engineering of Mondragon Unibertsitatea, where he is currently a Ph.D. Student. His current research interests include electrical machines vibration modelling and control.

Alex McCloskey was born in Dublin, Ireland. He received the B.Sc. and M.Sc. degrees in Mechanical Engineering and Industrial Engineering from Mondragon Unibertsitatea in 2009 and 2012 respectively. He developed his Ph.D. thesis about vibrations of electrical machines in Mondragon Unibertsitatea.

Since 2016, he has been with the Acoustics and Vibrations Group of the Mechanics and Manufacturing department of the Faculty of Engineering of Mondragon Unibertsitatea, where he is currently a Lecturer and Researcher. His current research interests include electrical machines design and diagnosis. He has participated in a number of research projects in the fields of elevator drives and railway traction.

Sergio Zarate was born in Vitoria-Gasteiz, Spain. He received the B.Sc., M.Sc. and Ph.D. degrees in Electrical Engineering from Mondragon Unibertsitatea, Mondragon, Spain, in 2012, 2014 and 2018, respectively.

Since 2018, he has been with the Electronics department of the Faculty of Engineering of Mondragon Unibertsitatea, where he is currently a Lecturer and Researcher. His current research interests include drives, electrical machines vibration and permanent magnet machine design and optimization.

Javier Poza was born in Bergara, Spain, in June 1975. He received the B.S. degree in Electrical Engineering from Mondragon Unibertsitatea, in 1999 and the Ph.D. degree in electrical engineering from the Institut National Polytechnique de Grenoble, Grenoble, France.

Since 2002, he has been with the Electronics department of the Faculty of Engineering of Mondragon Unibertsitatea, where he is currently an Associate Professor. His current research interests include electrical machine design, modelling, and control. He has participated in various research projects in the fields of wind energy systems, lift drives, and railway traction.